PROGRESS IN PHOTOVOLTAICS: RESEARCH AND APPLICATIONS
Prog. Photovolt: Res. Appl. 2008; **16**:461–466
Published online 3 March 2008 in Wiley InterScience (www.interscience.wiley.com) DOI: 10.1002/pip.823

Research

Surface Passivation of High-efficiency Silicon Solar Cells by Atomic-layer-deposited Al_2O_3

J. Schmidt[1]*,†, A. Merkle[1], R. Brendel[1], B. Hoex[2], M. C. M. van de Sanden[2] and W. M. M. Kessels[2]
[1]*Institut für Solarenergieforschung Hameln/Emmerthal (ISFH), Am Ohrberg 1, D-31860 Emmerthal, Germany*
[2]*Department of Applied Physics, Eindhoven University of Technology, P.O. Box 513, 5600 MB Eindhoven, The Netherlands*

Atomic-layer-deposited aluminium oxide (Al_2O_3) is applied as rear-surface-passivating dielectric layer to passivated emitter and rear cell (PERC)-type crystalline silicon (c-Si) solar cells. The excellent passivation of low-resistivity p-type silicon by the negative-charge-dielectric Al_2O_3 is confirmed on the device level by an independently confirmed energy conversion efficiency of 20·6%. The best results are obtained for a stack consisting of a 30 nm Al_2O_3 film covered by a 200 nm plasma-enhanced-chemical-vapour-deposited silicon oxide (SiO_x) layer, resulting in a rear surface recombination velocity (SRV) of 70 cm/s. Comparable results are obtained for a 130 nm single-layer of Al_2O_3, resulting in a rear SRV of 90 cm/s. Copyright © 2008 John Wiley & Sons, Ltd.

KEY WORDS: crystalline silicon solar cells; surface passivation; high-efficiency cells; aluminium oxide

Received 20 November 2007; Revised 8 January 2008

INTRODUCTION

The current trend in silicon-wafer-based photovoltaics towards thinner crystalline silicon (c-Si) wafers and higher efficiencies makes an effective reduction of surface recombination losses increasingly important. In high-efficiency laboratory silicon solar cells,[1–3] surface recombination is very effectively suppressed by means of silicon dioxide (SiO_2) grown in a high-temperature ($\geq$900°C) oxidation process. Very low surface recombination velocities (SRVs) are in particular realized at the lightly doped rear surface, where the combination of a thermally grown SiO_2 layer with an evaporated film of Al give—after an additional annealing treatment at ~400°C (the so-called 'alneal')—SRVs below 20 cm/s on unmetallized low-resistivity (~1 Ω cm) *p*-type c-Si wafers.[4] In addition, the SiO_2/Al stack at the cell rear acts as an excellent reflector for near-bandgap photons, significantly improving the light trapping properties and hence the short-circuit current of the cell. One of the main reasons why high-temperature oxidation has not been implemented into the majority of industrial cell processes up to now is the high sensitivity of the silicon bulk lifetime to high-temperature processes. In particular in the case of multi-c-Si wafers, thermal processes above 900°C typically lead to a significant degradation of the bulk lifetime.[5] Hence, low-temperature surface passivation alternatives are required for future industrial high-efficiency silicon solar cells, which should have comparable properties as the alnealed SiO_2. One intensively investigated alternative is silicon

* Correspondence to: J. Schmidt, Institut für Solarenergieforschung Hameln/Emmerthal (ISFH), Am Ohrberg 1, D-31860 Emmerthal, Germany.
†E-mail: j.schmidt@isfh.de

nitride (SiN_x), grown by plasma-enhanced chemical vapour deposition (PECVD) at ~400°C, which has proven to give comparably low SRVs as alnealed SiO_2 on low-resistivity *p*-type c-Si.[6,7] However, when applied to the rear of passivated emitter and rear cell (PERC)-type solar cells the short-circuit current density is strongly reduced compared to their SiO_2-passivated counterparts.[8] This effect has been attributed to the large density of fixed positive charges within the SiN_x layer, inducing an inversion layer in the c-Si underneath the SiN_x. The coupling of this inversion layer to the base contact leads to a significant loss in the short-circuit current density. This detrimental effect is known as 'parasitic shunting'.[9] Another alternative low-temperature passivation scheme resulting in comparable SRVs as alnealed SiO_2 is intrinsic hydrogenated amorphous silicon (a-Si) deposited by PECVD in the temperature range between 200 and 250°C.[10] Despite the fact that no parasitic shunting occurs in the case of an a-Si passivated cell rear, new problems arise from the high sensitivity of the a-Si passivation to thermal processes.

Recently, it was shown that thin films of aluminium oxide (Al_2O_3) grown by atomic layer deposition (ALD) provide an excellent level of surface passivation on *p*- and *n*-type silicon wafers, as determined from carrier lifetime measurements.[11,12] Using low-temperature plasma-assisted ALD SRVs <13 cm/s were demonstrated on low-resistivity *p*-type c-Si.[12] The fixed negative charge density within the Al_2O_3 layer induces an accumulation layer at the *p*-type c-Si surface that provides an effective field-effect passivation and the above-mentioned parasitic shunting effect at the solar cell rear is not expected. In combination with its very high transparency for near-bandgap photons, ALD-deposited Al_2O_3 should hence be an optimal choice for a dielectric layer at the c-Si solar cell rear. In this paper, we present first results of PERC-type solar cells with Al_2O_3-passivated rear surface, demonstrating the large potential of atomic-layer-deposited Al_2O_3 films for future high-efficiency silicon solar cells.

SOLAR CELL PROCESS

Figure 1 shows the PERC-type solar cell structure used in this study to demonstrate the applicability of Al_2O_3 rear surface passivation to high-efficiency silicon solar cells and Figure 2 shows the corresponding process flow diagram. As starting material we use (100)-oriented boron-doped float-zone (FZ) c-Si wafers with

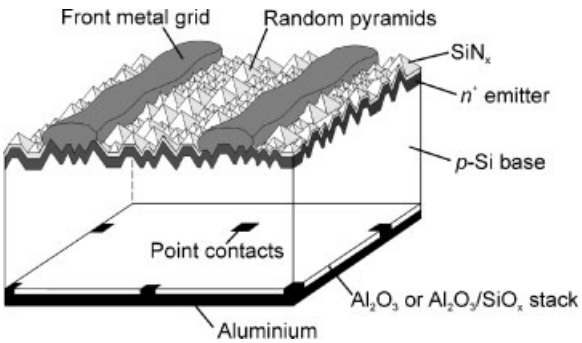

Figure 1. PERC-type solar cell structure used in this study to demonstrate the applicability of an Al_2O_3 rear surface passivation to high-efficiency solar cells

a thickness of 310 μm and a resistivity of 0·5 Ω cm. After damage etching of ~10 μm/side and wet chemical cleaning, an SiO_2 layer is grown on both wafer surfaces in a wet oxidation process at 1000°C. Subsequently, $2 \times 2\,cm^2$ diffusion windows are photolithographically opened on one wafer side and the silicon surface within the windows is textured with random pyramids in a KOH/isopropanol solution. A single-step phosphorus emitter is diffused from a $POCl_3$ source,[13] resulting in an n^+-emitter with a sheet resistance of 100 Ω/square, and the phosphorus glass is removed by a short HF dip. At this point of the process, the cell batch is split up into three batches, of which each one receives a different rear surface passivation: (i) one batch of cells keeps the thermally grown SiO_2, (ii) the second one is coated by a 130 nm Al_2O_3 film and (iii) the third batch is passivated by a stack consisting of a 30 nm Al_2O_3 layer and a 200 nm thick PECVD-SiO_x layer deposited in a Plasmalab 80+ parallel-plate reactor (Oxford Instruments) at 425°C. The Al_2O_3 films are deposited by plasma-assisted ALD in a commercial ALD reactor (FlexAL™, Oxford Instruments) at a deposition temperature of 200°C.[14] The plasma-assisted ALD Al_2O_3 process is split up into two self-limiting reactions consisting of a trimethyl-aluminium ($Al(CH_3)_3$) exposure and an O_2 plasma. The subsequent annealing step as applied in the study of Hoex *et al.*[11] is omitted in this case as adequate post-deposition annealing steps are already present in the process flow shown in Figure 2. The SiO_x layer is deposited in a continuous PECVD process using silane (SiH_4) and nitrous oxide (N_2O) as process gases. The remaining process steps are identical for all three cell batches. Using photolithography point contact openings are etched into the dielectric layers

DOI: 10.1002/pip

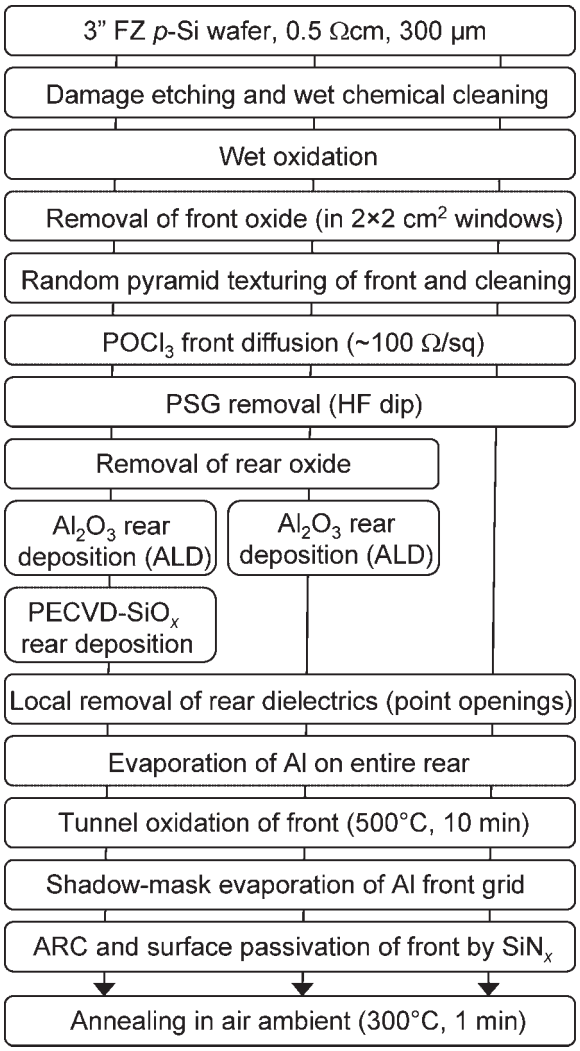

Figure 2. Process flow diagram for the PERC-type solar cells fabricated in this study

at the rear. A photolithography mask resulting in a point contact pitch of 2 mm and a metallization fraction of 4% is used. Twenty micrometre of aluminium is evaporated on the entire cell rear using electron-beam evaporation. A tunnel oxidation of the n^+-emitter is performed at 500°C for 10 min, resulting in an ~1·5 nm thick oxide layer.[15] The 20 μm thick Al front metal grid is then evaporated through a shadow mask onto the tunnel oxide. Finally, a surface-passivating SiN_x antireflection coating is deposited onto the front of the PERC solar cell by remote-PECVD at 300°C.[6] Before characterization all solar cells receive an additional 1-min 300°C anneal in air, which slightly improves the fill factor and the open-circuit voltage. The aperture area of all solar cells fabricated in this study is 4 cm^2 and the entire front metallization, including the busbar, is within the active cell area.

SOLAR CELL RESULTS

Table I summarizes the one-sun parameters of the processed PERC-type solar cells featuring different rear surface passivation schemes, as measured under standard testing conditions (25°C, 100 mW/cm^2, AM 1·5 G). The results marked with an asterisk were independently confirmed at Fraunhofer ISE CalLab. The best reference solar cell with alnealed SiO_2 rear surface passivation is characterized by an efficiency of $\eta = 20{\cdot}5\%$, an open-circuit voltage of $V_{oc} = 656$ mV and a short-circuit current density of $J_{sc} = 38{\cdot}9$ mA/cm^2. The analysis of the internal quantum efficiency (IQE) shows that the V_{oc} is limited by the front emitter. The average values of all four cells with SiO_2 rear

Table I. One-sun parameters measured under standard testing conditions of 290 μm thick PERC-type silicon solar cells with three different rear surface passivations: (i) thermal SiO_2 (220 nm), (ii) ALD-Al_2O_3 (130 nm) and (iii) ALD-Al_2O_3(30 nm)/PECVD-SiO_x(200 nm). All cells were fabricated on 0·5-Ωcm FZ *p*-Si wafers. The aperture cell area is 4 cm^2. Average values and standard deviations for all cells processed in the batch are also provided

Rear side	Cell ID	V_{oc} (mV)	J_{sc} (mA/cm^2)	FF (%)	η (%)
Thermal SiO_2 (220 nm)	7_1	656	38·9	80·3	20·5
	Average of 4	655 ± 1	38·4 ± 0·5	80·3 ± 1·3	20·2 ± 0·3
ALD-Al_2O_3 (130 nm)	3_3	655	38·7	78·9	20·0*
	Average of 4	656 ± 2	38·6 ± 0·1	79·4 ± 1·4	20·0 ± 0·4
ALD-Al_2O_3 (30 nm)/PECVD-SiO_x (200 nm)	2_4	660	39·0	80·1	20·6*
	Average of 8	657 ± 2	38·6 ± 0·3	80·4 ± 1·1	20·4 ± 0·4

*Calibrated measurement at Fraunhofer ISE CalLab.

DOI: 10.1002/pip

passivation show only a very small scatter, demonstrating the high reproducibility of the process. The average parameters of the cells with Al_2O_3, Al_2O_3/SiO_x and SiO_2 rear passivation agree within the scatter ranges. In particular it is noticeable that the J_{sc} of the cells with Al_2O_3 and Al_2O_3/SiO_x rear surface passivation is not reduced compared to the SiO_2-passivated cells. In the case of high-positive-charge dielectrics, such as SiN_x with fixed positive charge densities $>10^{12}\,cm^{-2}$, it was reported that J_{sc} is reduced by 1–2 mA/cm^2 compared to the thermal SiO_2 reference, due to the above-described parasitic shunting effect.[8,9] This effect is not expected in the case of Al_2O_3 as it is a negative-charge-dielectric inducing an accumulation layer instead of an inversion layer in the *p*-type c-Si underneath the rear surface. Al_2O_3 films are generally characterized by a high fixed negative charge density up to $-10^{13}\,cm^{-2}$.[11,16] The cell results summarized in Table I confirm the expected non-existence of the parasitic shunting for Al_2O_3-passivated as well as for Al_2O_3/SiO_x-passivated rear surfaces. The best cell of the entire batch is obtained for the Al_2O_3/SiO_x-passivated cell, resulting in an independently confirmed efficiency of $\eta = 20{\cdot}6\%$, a V_{oc} of 660 mV and a J_{sc} of 39·0 mA/cm^2.

It is not possible to quantify the exact rear surface passivation quality from comparison of the cell parameters given in Table I, as these solar cells are largely limited by recombination losses in the front emitter. Hence, we analyse the IQE in the wavelength range 800–1200 nm to determine the rear SRVs of the different rear surface passivation schemes. The symbols in Figure 3 show the IQE as a function of wavelength λ of three representative PERC cells with the different rear passivation schemes, measured at a fixed bias light intensity of 0·3 suns. The solid lines in Figure 3 show the fits to the measured data. To model the IQE(λ) dependence we use the software LASSIE,[17,18] which combines the extended IQE evaluation by Basore[19] with the improved optical model developed by Brendel.[20] The bulk lifetime is assumed to be limited by Auger recombination, resulting in a bulk diffusion length of $L_b = 1500\,\mu m$ for the $0{\cdot}5\,\Omega\,cm$ *p*-type silicon material used in this work.[21] As we assume the intrinsic upper limit for the bulk lifetime, the SRVs determined from the IQE analysis are upper limits as well. Table II summarizes the rear SRVs S_r and the internal rear reflectances R_r extracted from the IQE analysis. All three rear structures are equally effective reflectors for near-bandgap photons ($R_r = 91\%$). The rear SRV of the reference cell with

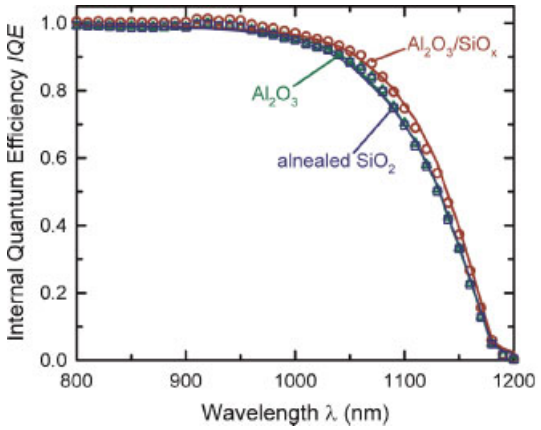

Figure 3. Measured internal quantum efficiency IQE as a function of wavelength λ (symbols) for solar cells with three different rear surface passivations: (i) thermal SiO_2 (220 nm), (ii) ALD-Al_2O_3 (130 nm) and (iii) ALD-Al_2O_3(30 nm)/PECVD-SiO_x(200 nm). The lines show the fitted IQE(λ) curves. All measurements were taken with a white bias light intensity of ∼0·3 suns

alnealed SiO_2 amounts to $S_r = (90 \pm 20)$ cm/s. The extracted S_r for the cell with single-layer Al_2O_3 rear passivation is the same as for the SiO_2-passivated reference cell, showing that ALD-deposited Al_2O_3 performs as good as aluminium-annealed high-temperature-grown SiO_2. A further reduction in the S_r is obtained for the Al_2O_3/SiO_x stack, resulting in an S_r of only (70 ± 20) cm/s, which we attribute to the hydrogenation of interface states at the Al_2O_3/Si interface during deposition of the hydrogen-rich SiO_x layer.

The effective SRV of a point-contacted rear is given by Fischer's equation:[18]

$$S_r = \frac{D_n}{W}\left[\frac{p}{2W\sqrt{\pi f}}\arctan\left(\frac{2W}{p}\sqrt{\frac{\pi}{f}}\right) - \exp\left(-\frac{W}{p}\right) + \frac{D_n}{fWS_{met}}\right]^{-1} + \frac{S_{pass}}{1-f} \quad (1)$$

where D_n is the electron diffusion coefficient, W the wafer thickness, p the contact pitch, f the metallization fraction and S_{met} and S_{pass} are the SRVs on the metallized and on the passivated areas of the rear, respectively. Equation (1) holds for arbitrary values of S_{met} as long as low-injection conditions prevail. It

DOI: 10.1002/pip

Table II. Effective rear surface recombination velocity S_r and internal rear reflectance R_r extracted from the IQE measurements shown in Figure 3

Rear side	Rear surface recombination velocity S_r (cm/s)	Internal rear reflectance R_r (%)
Thermal SiO_2 (220 nm)	90 ± 20	91 ± 1
Al_2O_3 (130 nm)	90 ± 20	90 ± 1
Al_2O_3 (30 nm)/SiO_x (200 nm)	70 ± 20	91 ± 1

has been verified experimentally on lifetime test structures[22] as well as on solar cells.[23] According to Equation (1) the minimum SRV $S_{r,min}$ for a point-contact rear with perfect passivation in the non-metallized area (i.e. $S_{pass} = 0$) is given by the first summand on the right-hand side of Equation (1). For our cell structure we determine $S_{r,min} = 73$ cm/s ($D_n = 23$ cm^2/s, $W = 290$ μm, $p = 2000$ μm, $f = 4\%$, $S_{met} \geq 10^5$ cm/s), clearly demonstrating that in the case of the Al_2O_3/SiO_x stack, recombination in the passivated area of the cell rear can be completely neglected. Note that, although a slightly better passivation is obtained in the case of the Al_2O_3/SiO_x stacks, the rear SRV of the single-layer Al_2O_3-passivated cells is also for the most part determined by recombination at the metal contacts. The IQE results clearly prove that atomic-layer-deposited Al_2O_3 is a very effective new dielectric passivation layer for high-efficiency silicon solar cells.

CONCLUSIONS

We have demonstrated that Al_2O_3 films deposited by plasma-assisted ALD are suitable for the surface passivation of point-contacted rear surfaces of high-efficiency solar cells. Independently confirmed efficiencies above 20% have been obtained for PERC-type solar cells with the point-contacted rear passivated by a 130 nm Al_2O_3 layer as well with a double layer consisting of a 30 nm Al_2O_3 film and a 200 nm PECVD-SiO_x layer. IQE measurements have revealed that the effective surface recombination velocities of the single-layer Al_2O_3-passivated cells are comparable and that of the Al_2O_3/SiO_x-passivated cells are even below that measured on reference cells passivated by an alnealed thermal SiO_2. The measured effective rear surface recombination velocities of all cells were shown to be clearly dominated by recombination at the metal point contacts.

In addition to the excellent surface passivation provided by Al_2O_3 films deposited by plasma-assisted ALD, the deposition process itself is also beneficial from an application point of view. In contrast to the conventionally applied PECVD, ALD consists of two self-limiting half-reactions, which implies several advantages: (i) ALD gives highly conformal coatings, which allows to deposit and passivate for example deep trenches or even pores in silicon, (ii) pin-hole and particle free deposition is achieved, (iii) as ALD is a self-limiting process uniform films can be deposited over large areas with mono-layer growth control and (iv) very low impurity concentrations of deposited films and hence very high film quality is achieved. The main disadvantage of ALD for photovoltaic applications is its relatively low deposition rate. However, as shown in this study, this disadvantage can be overcome by depositing ultrathin (2–30 nm) ALD-Al_2O_3 films and capping them with a thicker film of for example PECVD-SiO_x. Apart of the advantageous optical properties of these stacks, we have demonstrated that the passivation quality of such ALD-Al_2O_3/PECVD-SiO_x stacks can even be superior to that of single layers of Al_2O_3, which we attribute to the hydrogenation of interface states at the Al_2O_3/Si interface during deposition of the hydrogen-rich SiO_x layer. The same beneficial effect is expected from other hydrogen-rich PECVD-deposited films such as SiN_x or SiC_x. Combination of ALD and PECVD might hence be a key technology for future industrial high-efficiency solar cells.

Acknowledgements

The authors thank all members of the photovoltaic groups at ISFH for their contributions to this work and W. Keuning (Eindhoven University of Technology) for carrying out the Al_2O_3 depositions. We gratefully acknowledge the financial support provided by the German State of Lower Saxony and the Netherlands Technology Foundation STW.

DOI: 10.1002/pip

REFERENCES

1. Green MA, Blakers AW, Zhao J, Milne AM, Wang A, Dai X. Characterization of 23-percent efficient silicon solar cells. *IEEE Transactions on Electronic Devices* 1990; **37**: 331–336.
2. Aberle A, Warta W, Knobloch J, Voß B. Surface passivation of high efficiency silicon solar cells. *Proceedings of the 21st IEEE Photovoltaic Specialists Conference*, 1990; 233–238.
3. Zhao J, Wang A, Green MA. 24.5% efficiency silicon PERT cells on MCZ substrates and 24.7% efficiency PERL cells on FZ substrates. *Progress in Photovoltaics* 1999; **7**: 471–474.
4. Kerr MJ, Cuevas A. Very low bulk and surface recombination in oxidized silicon wafers. *Semiconductor Science and Technology* 2001; **17**: 35–38.
5. Stocks MJ, Cuevas A, Blakers AW. Minority carrier lifetimes of multicrystalline silicon during solar cell processing. *Proceedings of the 14th European Photovoltaic Solar Energy Conference*, Barcelona, Spain, 1997; 770–773.
6. Lauinger T, Schmidt J, Aberle AG, Hezel R. Record low surface recombination velocities on 1 Ω cm *p*-type silicon using remote plasma silicon nitride passivation. *Applied Physics Letters* 1996; **68**: 1232–1234.
7. Schmidt J, Moschner JD, Henze J, Dauwe S, Hezel R. Recent progress in the surface passivation of silicon solar cells using silicon nitride. *Proceedings of the 19th European Photovoltaic Solar Energy Conference*, Paris, France, 2004; 391–396.
8. Dauwe S, Mittelstädt L, Metz A, Schmidt J, Hezel R. Low-temperature rear surface passivation schemes for >20% efficient silicon solar cells. *Proceedings of the 3rd World Conference on Photovoltaic Energy Conversion*, Osaka, Japan, 2003; 1395–1398.
9. Dauwe S, Mittelstädt L, Metz A, Hezel R. Experimental evidence of parasitic shunting in silicon nitride rear surface passivated solar cells. *Progress in Photovoltaics* 2002; **10**: 271–278.
10. Dauwe S, Schmidt J, Hezel R. Very low surface recombination velocities on *p*- and *n*-type silicon wafers passivated with hydrogenated amorphous silicon films. *Proceedings of the 29th IEEE Photovoltaic Specialists Conference*, New Orleans, USA, 2002; 1246–1249.
11. Agostinelli G, Delabie A, Vitanov P, Alexieva Z, Dekkers HFW, De Wolf S, Beaucarne G. Very low surface recombination velocities on p-type silicon wafers passivated with a dielectric with fixed negative charge. *Solar Energy Materials and Solar Cells* 2006; **90**: 3438–3443.
12. Hoex B, Heil SBS, Langereis E, van de Sanden MCM, Kessels WMM. Ultralow surface recombination of c-Si substrates passivated by plasma-assisted atomic layer deposited Al_2O_3. *Applied Physics Letters* 2006; **89**: 042112/1-3.
13. Hübner A, Hampe C, Aberle AG. A simple fabrication process for 20% efficient silicon solar cells. *Solar Energy Materials and Solar Cells* 1997; **46**: 67–77.
14. van Hemmen JL, Heil SBS, Klootwijk J, Roozeboom F, Hodson CJ, van de Sanden MCM, Kessels WMM. Plasma and thermal ALD of Al_2O_3 in a commercial 200 mm ALD reactor. *Journal of the Electrochemical Society* 2007; **154**: G165–G169.
15. Hezel R, Metz A. Crystalline silicon solar cells with efficiencies above 20% suitable for mass production. *Proceedings of the 16th European Photovoltaic Solar Energy Conference*, Glasgow, UK, 2000; 1091–1094.
16. Hezel R, Jaeger K. Low-temperature surface passivation of silicon for solar cells. *Journal of the Electrochemical Society* 1989; **136**: 518–523.
17. www.fischer-pv.de
18. Fischer B. *Loss analysis of crystalline silicon solar cells using photoconductance and quantum efficiency measurements*, Ph.D. thesis, University of Konstanz, 2003.
19. Basore PA. Extended spectral analysis of internal quantum efficiency. *Proceedings of the 23rd IEEE Photovoltaic Specialists Conference*, 1993; 147–152.
20. Brendel R, Plieninger R. IQE1D—a computer program for routine quantum efficiency analysis. *Technical Digest of the 9th International Photovoltaic Science and Engineering Conference*, Miyazaki, Japan, 1996; 521–522.
21. Altermatt PP, Schmidt J, Heiser G, Aberle AG. Assessment and parameterisation of Coulomb-enhanced Auger recombination coefficients in lowly injected crystalline silicon. *Journal of Applied Physics* 1997; **82**: 4938–4944.
22. Plagwitz H, Schaper M, Schmidt J, Terheiden B, Brendel R. Analytical model for the optimization of locally contacted solar cells. *Proceedings of the 31st IEEE Photovoltaic Specialists Conference*, Orlando, USA, 2005; 999–1002.
23. Kray D, Glunz SW. Investigation of laser-fired rear-side recombination properties using an analytical model. *Progress in Photovoltaics: Research and Applications* 2006; **14**: 195–201.

DOI: 10.1002/pip